Lan, Yifu; Lin, Weiwei; Zhang, Youqi

Bridge frequency identification using vibration responses from sensors on a passing vehicle

Published in:
Bridge Safety, Maintenance, Management, Life-Cycle, Resilience and Sustainability

DOI:
10.1201/9781003322641

Published: 26/06/2022

Document Version
Peer-reviewed accepted author manuscript, also known as Final accepted manuscript or Post-print

Bridge frequency identification using vibration responses from sensors on a passing vehicle

Y. Lan, W. Lin & Y. Zhang
Department of Civil Engineering, School of Engineering, Aalto University, Espoo, Finland

ABSTRACT: This paper introduces a coherence-based signal processing strategy to identify the natural bridge frequency from acceleration responses of different sensors mounted on a vehicle passing through a bridge. Natural frequencies are fundamental dynamic characteristics of bridges, and it is theoretically feasible to identify natural frequencies of bridges from vehicle vibration responses. However, applying the vehicle-based measurement approach in practice still has difficulties as the vehicle responses always involve complex and varied components. In engineering practice, non-bridge frequency peaks in conjunction with a weak bridge frequency peak would be a very common scenario leading to deceptive frequency identification. The coherence index, which can be obtained using the cross-spectrum estimation, is employed in this study to represent the correlation among different vehicle signals. Instead of employing multiple vehicle systems or extremely heavy cars as excitation sources in previous studies, the proposed method only requires one equipped normal vehicle for the bridge frequency estimation. The effectiveness of the proposed method is validated by diverse bridge situations in an experimental environment, demonstrating good performances. The presented coherence index is sensitive to bridge frequency changes and has high recognizability, which is practically applicable to the smart monitoring system to automate the detection process.

1 INTRODUCTION

Natural frequency is one of the most fundamental characteristics of bridges, reflecting bearing conditions and characterizing resonance phenomena under periodic loading (Salawu 1997). It is a commonly used indicator for diagnosing bridge health conditions, while the extraction of bridge natural frequencies is usually difficult in practice. Conventionally, the bridge natural frequency is identified using sensors installed on the structure directly, also known as "sensor-based monitoring systems" (Sohn et al. 2003). The sensor installation on bridges is expensive, unsafe and laborious, particularly for a bridge under ongoing traffic or in a dangerous location (Enckell et al. 2011). Moreover, sensors mounted on the bridge are greatly susceptible to be damaged due to environmental factors such as weather, resulting in substantial repair and maintenance expenses (Kim et al. 2006). Furthermore, because the instrumentation is permanently installed on the bridge as a customized SHM framework, it is difficult to transfer one monitoring system to other bridges (Elhattab et al. 2016). These disadvantages limit the widespread application of traditional SHM methods on bridges in general.

The drive-by bridge inspection approach, an indirect SHM technique, has been increasingly prominent as a study topic in recent years (Cantero et al. 2019). Studies have investigated the potentials of employing the drive-by inspection method to obtain essential information of bridges (Nguyen & Tran 2010, Miyamoto & Yabe 2012, Cerda et al. 2014, Obrien et al. 2014, Obrien & Keenahan 2015, Obrien et al. 2017, Nagayama et al. 2017, Lan 2021, Lan 2021). The bridge vibrates when vehicles pass through it, and the dynamic information of the bridge will be reflected in vehicle responses via the Vehicle-Bridge Interaction (VBI) procedure, in which the vehicle performs as a "moving sensor" (Hester & González 2017, Wang et al. 2017). Such an approach, therefore, does not require numerous instrumentations to be placed on the bridge but only a few sensors on the passing vehicle (Yang et al. 2014). The indirect SHM method provides advantages in mobility, economy, and efficiency when compared to traditional techniques (Malekjafarian et al. 2015).

Although it is theoretically possible to extract the bridge natural frequency from the VBI process, the vehicle-based measurement is typically difficult to conduct in engineering practice. Vehicle and bridge models that have been used in previous studies are generally oversimplified or customized, which are distant from realistic situations. As cars with customized qualities, like excessively heavy weight (over 8% of bridge mass) and close-to-bridge frequency, would lead to intense VBI responses, thus significantly strengthening the bridge frequency components in vehicle spectrogram (Green & Cebon 1997). In reality, though, such tailored vehicles are rarely available. The spectral peak associated with the bridge frequency might be small in practice, and the interference from roughness components or vehicle dynamics could obscure the signal of interest. Non-bridge frequency peaks in conjunction with a weak bridge frequency peak (or none at all) would be very common, and this could lead to a misidentification of natural frequencies (Yang & Yang 2018). A practical approach for identifying the bridge frequency among others in normal VBI situations is required.

This paper presents a novel strategy to identify the bridge frequency by using multiple accelerometers on a passing truck. Customized cars or multiple vehicle systems are not necessary required to emphasize the bridge vibration components; instead, a commercial truck with sensors installed at various locations is used. It converts the frequency identification problem into a coherence-related problem, where the coherence indexes are computed by using cross-spectral density function estimation to distinguish the bridge-related frequency peak. The feasibility of the strategy is examined by laboratory experiments with a truck model and a steel beam. This experimental model can largely reconstruct a regular VBI scene, when a real-scaled commercial truck model with an engine system is employed. The bridge natural frequency is identified under various bridge cases with a fully loaded truck, demonstrating the performance of the presented technique.

2 BRIDGE FREQUENCY IDENTIFICATION ALGORITHM

Vibration signals received from sensors on the vehicle always contain complicated and varied components. Bridge-related components in the spectrum are usually smaller than those associated with vehicle dynamics and other noises, making it difficult to distinguish the bridge frequency from others. Multiple or specialized vehicle systems, which have been widely employed in prior research to emphasize the components associated to bridge frequency, are not always accessible. On the other hand, it is found that the bridge vibration component appears commonly in the responses of car sensors placed on different positions, while signal components from noises are less identical. As vehicle parts always have different structures and mechanisms (e.g., rear axle and the container) even within the same car. The bridge vibration will occur in all parts as the common excitation, but vibration signals containing a random nature like road profiles will be damped or disturbed by vehicle mechanisms, showing less relevant features.

This section describes a coherence-based signal processing strategy to identify the natural bridge frequency from vehicle cross-spectrums. Four sensors are used in the study to simultaneously capture the vertical acceleration responses of the truck travelling through the bridge. They are mounted on the front of a car, front axle, rear axle and container, respectively, to provide required signals to the strategy. This requires the application of cross-spectrum estimation proposed by Bendat and Piersol (2011):

$$R_{fg}(\tau) = \int_{-\infty}^{\infty} f^*(t)g(t+\tau)dt \quad (1)$$

$$G_{xy}(f) = \mathcal{F}[R_{fg}(\tau)] \quad (2)$$

where $R_{fg}(\tau)$ is the cross-correlation function of two random processes $f(t)$ and $g(t)$; the asterisk * denotes complex conjugate; and τ is the time displacement. $G_{xy}(f)$ represents the cross-spectral density function; and $\mathcal{F}$ is defined as the Fourier transform.

Employing the cross-spectrum estimation, the algorithm is described as follows:

1. Obtain vertical acceleration signals of the vehicle, i.e. $\ddot{y}_a$, $\ddot{y}_b$, $\ddot{y}_c$ and $\ddot{y}_d$ from sensors on the front of the car, front axle, rear axle and the container, respectively.

2. Use $\ddot{y}_c$ and $\ddot{y}_a$, $\ddot{y}_c$ and $\ddot{y}_b$, $\ddot{y}_c$ and $\ddot{y}_d$, respectively, as the random processes $f(t)$ and $g(t)$, to compute the cross-spectral density function.

3. The coherence indexes, $C_1(f_i)$, $C_2(f_i)$, $C_3(f_i)$, are solved by three positioning combinations within the frequency range of interest, in which the rear axle is used as a reference. The rear axle, which served as the load-carrying axle, is usually assumed to be the most sensitive to the bridge vibration.

The coherence index is then calculated by combining the three indexes:

$$C(f_i) = C_1(f_i) + C_2(f_i) + C_3(f_i) \quad (3)$$

Where the peak *i* is deemed prominent when its corresponding index is greater than a threshold; the threshold is empirically determined as 1.6 in this study.

4. For a fully loaded truck, the bridge natural frequency is recognized by finding the largest coherence indexes, $C(f_i)$, and excluding the vehicle frequency itself. The "dynamic frequency" of a driving vehicle naturally has the largest vibration commonality within the vehicle system. The 1st mode frequency of the bridge is identified as the greatest frequency peak in the cross-spectrum just after the truck's frequency. Figure 1 shows a schematic illustration of the present strategy's method.

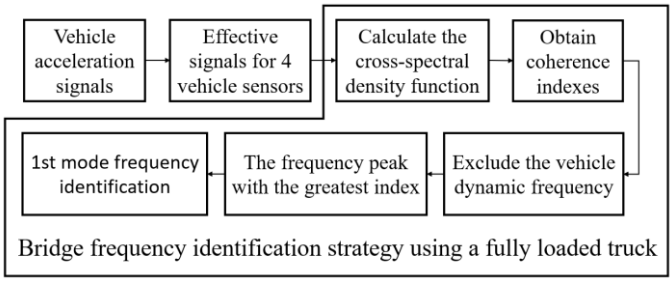

Figure 1. Schematic illustration of the present strategy.

3 EXPERIMENTAL PROGRAM

Laboratory experiments are carried out to verify the present technique. The bridge frequency is modified by placing extra weights on the bridge with different mass sizes and locations, which in fact could represent structural damages in various positions and severities as in previous studies (Cerda et al. 2014, Kim et al. 2014, Zhang et al. 2019, Zhang et al. 2019, Liu et al. 2020).

3.1 *Bridge model setup*

A HEA400 simply supported steel beam was utilized to model a bridge in the experiment as shown in Figure 2. The following are the physical properties of the steel beam: elastic modulus E = 210 GPa; density ρ = 7.85 × 10^3 kg/m^3; length L = 4 m; section area A = 15898 mm^2 and moment of inertia I = 85.64 × 10^6 mm^4. The fundamental natural frequency of a simply supported beam can be computed by:

$$f_{\mathrm{b}}^{(1)} = \frac{1}{2\pi}\left(\frac{\pi}{L}\right)^2 \sqrt{\frac{EI}{m}} \tag{4}$$

where m represents the mass per unit length of the bridge; and the bridge natural frequency is theoretically estimated as 36.3 Hz.


Figure 2. Steel beam used as a bridge model.

The experimental setup contains an acceleration ramp and a deceleration ramp. As artificial damages, various-sized masses are added to three positions, altering the bridge frequency. Three accelerometers are installed on the steel beam at 0.1L, 0.5L, and 0.9L, respectively, to collect bridge vibrations during the vehicle passage. The details of the experimental setup are shown in Figure 3.

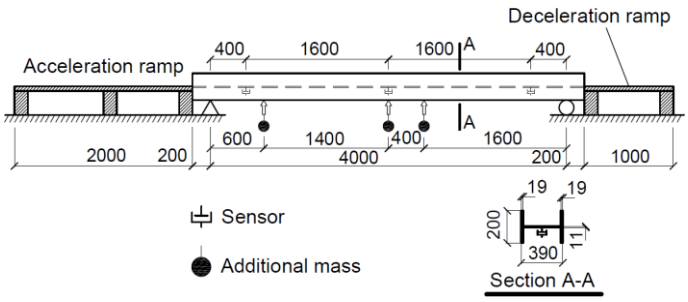

Figure 3. Details of the experimental beam model setup.

Figures 4a and 4b show how the mass and the sensor are attached to the beam. The PC-driven data acquisition system is connected to sensors via cables, which provides a sampling rate of 2000Hz. Data from bridge sensors, as the real bridge vibration responses, will be compared to car responses.

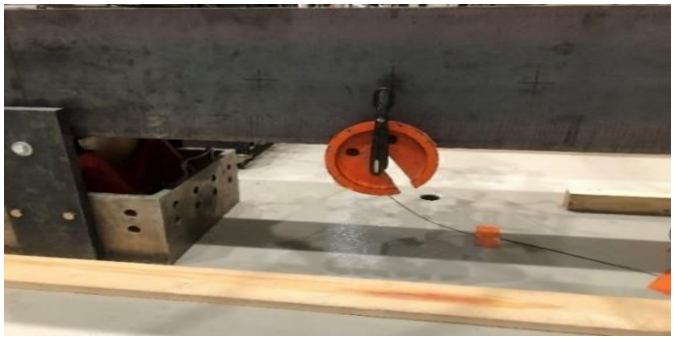
(a) Placement of the additional mass.


(b) Installation of the accelerometer.
Figure 4. Attachments on the beam.

3.2 *Vehicle model setup*

As presented in Figure 5, Tamiya's Mercedes-Benz 1850L is employed as the car model in the experiment. The configuration and mechanics of the full-sized truck are realistically captured in this 1/14 scaled car model (568mm×202mm). The weight of the vehicle itself is 4.05 kg based on the laboratory measurement, which is about 0.8% of the bridge

mass. Four sensors are instrumented at the front of the car, front axle, rear axle and the container, respectively, as shown in Figures 6a, b.

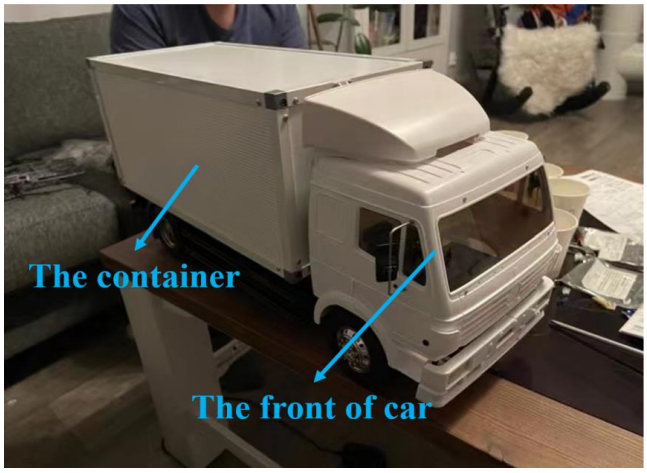

Figure 5. Scaled truck model.

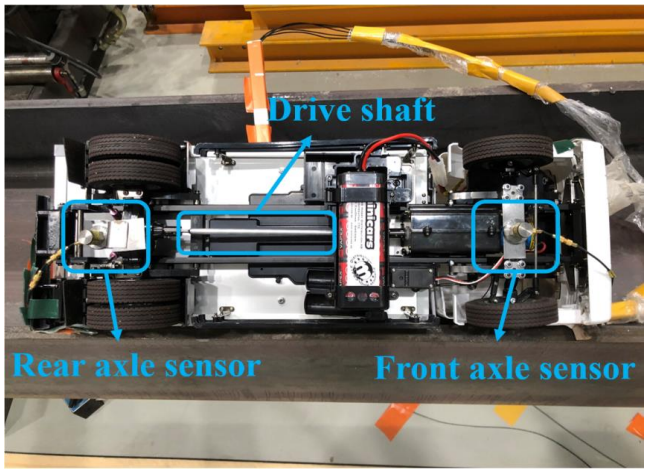

(a) Bottom truck.

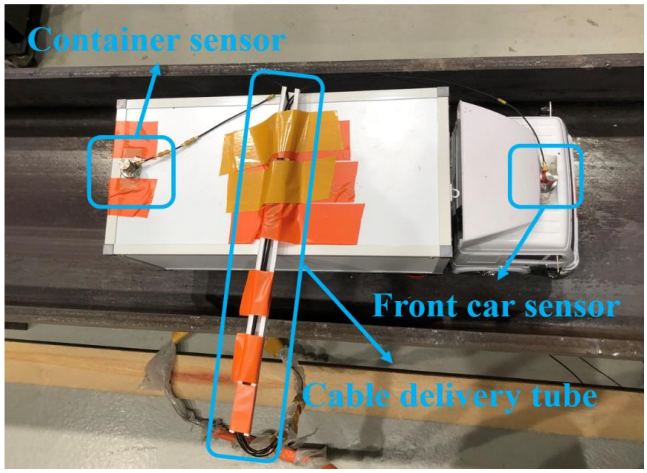

(b) Top truck.
Figure 6. Sensor installation.

In the experiment, loading weights of 6kg are placed inside the container, as depicted in Figure 7a, to simulate the "fully loaded" situation of the truck. The truck is driven by a 540-brushed type motor operated by an electronic controller as shown in Figure 7b. It is controlled to pass across the beam at a relatively constant and low speed of nearly 1 m/s.


(a) (b)
Figure 7. (a) Loading weights inside the container, (b) Electric controller.

3.3 *Experimental method*

The employed experimental models, just like many realistic cases, would not cause significant VBI responses. Such models can examine the present methodology more effectively and provide references to practical problems. Firstly, the proposed strategy is tested for the original bridge condition to demonstrate the computing process. Secondly, the bridge frequency is modified by adding masses of 20kg, 10kg, 5kg to 0.6m, 2m and 2.4m of the beam in sequence, as indicated in Table 1. Thirdly, the fully loaded truck is controlled to travel through the beam under the above 10 cases, containing the original state, and 7 crossings are repeated for each case.

Table 1. Bridge case description.

Case No.	Location	Weight	Case No.	Location	Weight
1	0	0	6	2 m	10 kg
2	0.6 m	20 kg	7	2 m	5 kg
3	0.6 m	10 kg	8	2.4 m	20 kg
4	0.6 m	5 kg	9	2.4 m	10 kg
5	2 m	20 kg	10	2.4 m	5 kg

4 RESULTS AND ANALYSIS

4.1 *Acceleration acquisition and signal processing*

Figure 8 shows the vertical acceleration signals of the passing truck under the original bridge condition. The dash line "I" in the figure indicates the front axle enters the bridge; the rear axle accesses the bridge at dash line "II"; responses at line "III" show that the front axle leaves the beam while the dash line "IV" shows the rear axle passing the beam. Due to the unsmooth transition between the accelerating ramp and the steel beam, there is a peak in the signal response of the front axle when the truck enters the bridge.

Similarly, a peak in the acceleration records of the front axle can also be found when it leaves the beam. Meanwhile, the bouncing and pitching motions induced by the rear axle traversing the bridge will be communicated to the front axle due to coupling effects in the car itself. The entrance/exit information of the rear axle can also be seen at the front axle (the peaks following "I" and "III"). The effective signals in the study are selected as the acceleration signals between dash lines "II" and "III", when the entire truck is on the beam.

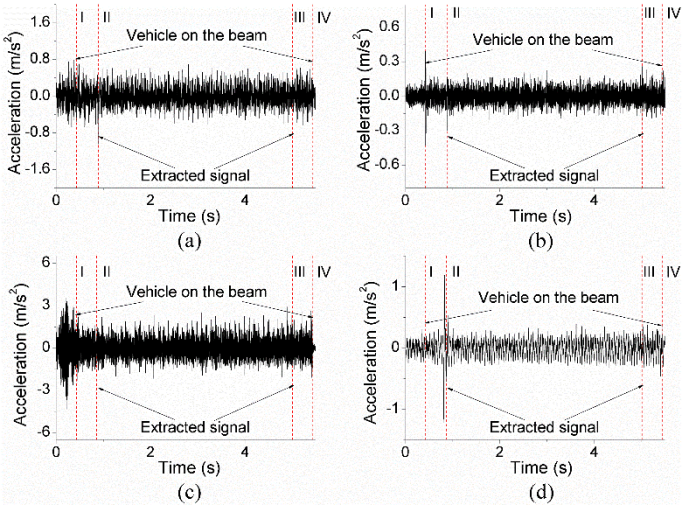

Figure 8. Original acceleration signals from vehicle sensors in different locations: (a) Front of the car, (b) Front axle, (c) Rear axle, (d) Container.

The Fast Fourier Transforms (FFT) of acceleration data from four sensor positions (e.g. front car, front axle, rear axle, and container) on the truck, ranging from 0 to 100 Hz, are shown in Figures 9a, b, c, d. While the actual bridge natural frequency is derived from the FFT of bridge sensor responses within the range from 0 to 100Hz, as presented in Figure 10, which is 35.3 Hz, somewhat different from the theoretically estimated result of 36.3Hz. The bridge frequency is more prominent in axel measurements, and this supports the findings of Koski et al. (2021). In engineering practice, however, this frequency value is supposedly unrecognized or only a broad range is known. The commonly used method of directly obtaining the bridge natural frequency from the vehicle spectrum is only applicable when the bridge frequency noticeably dominates the spectrum, which can often be found under strong VBI responses.

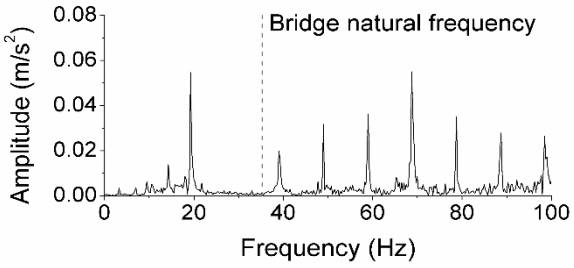

(a) The front car.

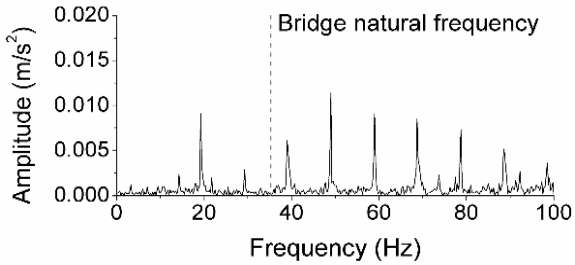

(b) The front axle.

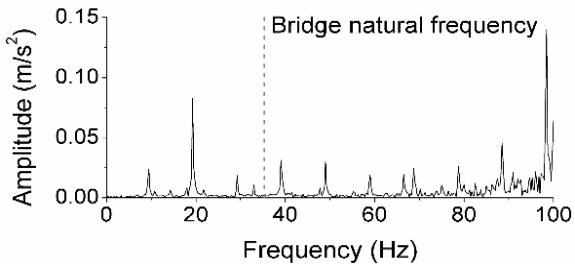

(c) The rear axle.

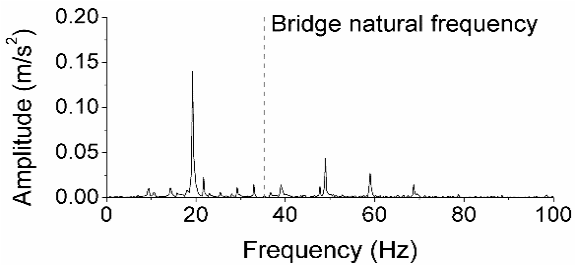

(d) The container.

Figure 9. FFT of acceleration signals from sensors at different locations.

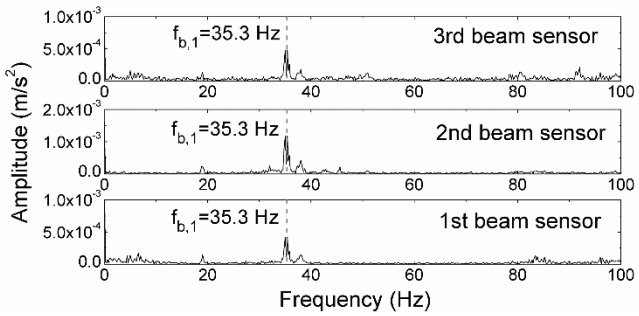

Figure 10. FFT of acceleration signals of bridge sensors.

4.2 *Strategy performance for the original bridge case*

The cross-spectrums derived from the responses of vehicle sensors and their sum, coherence index, for the above case are shown in Figures 11a, b, respectively, using the suggested strategy in cross-spectrum estimation. The first three prominent peaks with substantial commonality are marked in Figure 11b, and Table 2 shows the values of $C(f_i)$ with their components of $C_1(f_i)$, $C_2(f_i)$ and $C_3(f_i)$ for i = {1, 2, 3}. At a speed of 1 m/s, the vehicle dynamic frequency is 19.5 Hz, and its coherence index is calculated as 2.95 using cross-spectrum estimation, marked as the first prominent peak, f_1. Excluding the vehicle dynamic frequency, f_1, in the cross-spectrum, observably the frequency peak, f_2, has the highest coherence index

of 2.77, representing the most common vibration component in the vehicle system except for the vehicle frequency itself. The bridge natural frequency is consequently chosen as f_2, which is 39.0Hz, with a difference of 3.7Hz (10.4%) from the actual bridge frequency (35.3Hz).

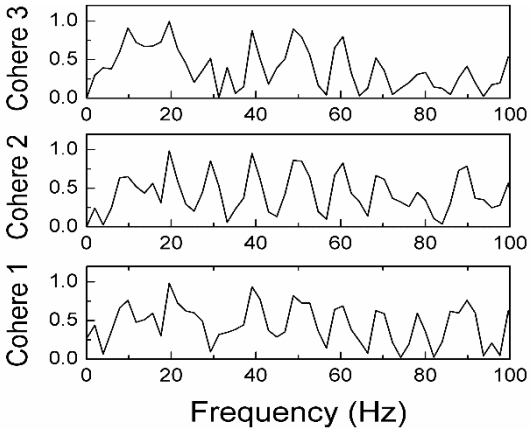

(a) Cohere 1: rear axle – front car; cohere 2: rear axle – front axle; cohere 3: rear axle – container.

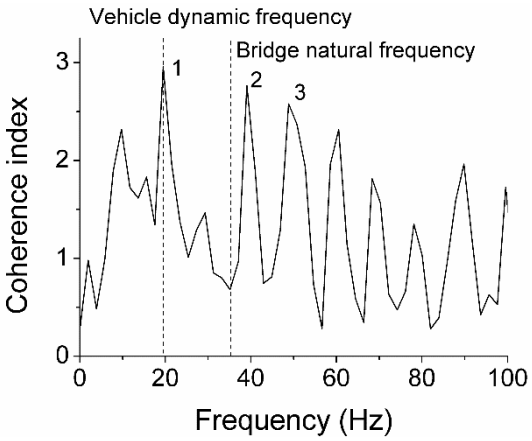

(b) Vehicle coherence index.

Figure 11. Cross-spectrums.

Table 2. Coherence indexes for the "Original" bridge case.

i	1	2	3
f_i (Hz)	19.5	39.0*	48.8
$C_1(f_i)$	0.98	0.95	0.86
$C_2(f_i)$	0.98	0.94	0.82
$C_3(f_i)$	0.99	0.88	0.89
$C(f_i)$	2.95	2.77	2.57

* The bridge frequency identified by the vehicle cross spectrum.

The first two prominent peaks (19.5 & 39.0Hz) remain the same when the cross-spectrum is focused on the whole frequency range from 0 to 1000Hz, as indicated in Figure 12a. Similar results can be seen if the vehicle is exposed to the full loading weight of 6kg. These show that the proposed strategy could identify the bridge-related frequency over a broad frequency range when heavy loads are applied to the truck, which is important in cases when the determination of a rough frequency range is challenging.

The cross-spectrum corresponding to the coherence index calculated by the rear axle and the mid-span bridge is presented in Figure 12b, which confirms the identification results. It demonstrates that the truck and the bridge system do share common frequency components with large coherence indexes. It is worth mentioning that, in Figure 12b, the third prominent peak approaches the 2nd mode frequency of bridge (148.9 Hz), while the first and second peaks are identical to the vehicle cross-spectrum. The presence of the 2nd mode frequency, on the other hand, is less common in various vehicle components, and the third prominent peak in the vehicle cross-spectrum has no evident physical explanation, implying that the suggested technique may not perform well in the high-mode bridge frequency estimation.

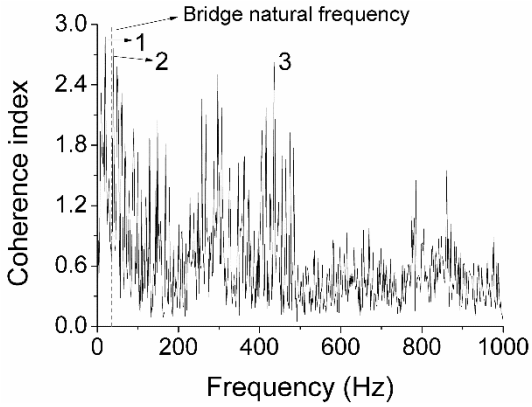

(a) Vehicle system.

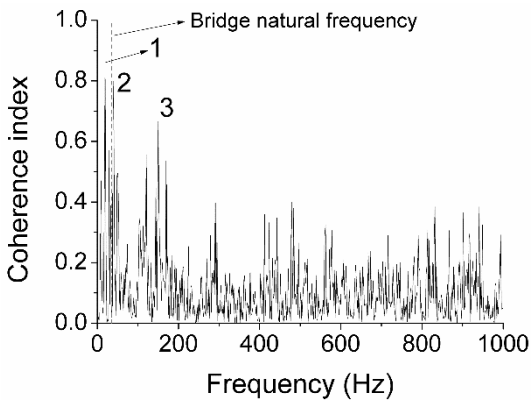

(b) Rear axle – mid-span bridge.

Figure 12. Coherence index.

4.3 *Results for diverse bridge frequency cases*

The performance of the proposed strategy is tested by various frequency cases, where the bridge natural frequency is changed by adding extra masses of different sizes and positions. Table 3 summarizes the frequency estimation results with 10 cases of diverse bridge conditions (7 passages for each case). $\bar{f}_{b,1}$ is the actual bridge natural frequency obtained from the bridge accelerometer, while $\hat{f}_{b,1}$ represents the frequency value estimated by the proposed strategy.

They are the average values for multiple passages in each case. Frequency Shift is the difference between the estimated and the real bridge frequency, $|\bar{f}_{b,1} - \hat{f}_{b,1}|$. The discrepancy, $\Delta f_{b,1}$, in the study is given by:

$$\frac{|\bar{f}_{b,1} - \hat{f}_{b,1}|}{\bar{f}_{b,1}} \times 100\% \quad (5)$$

The results reveal that the present technique can successfully identify the bridge natural frequency despite the occurrence of frequency shifts. The frequency shifts between 3.4 Hz and 3.7 Hz, and the discrepancy varies from 9.8% to 10.9%. This is because the energy transmission in diverse mediums is always accompanied by energy dispersion, similar to Doppler's effect. The frequency shift will be maintained in a specified range for certain media, such as the steel beam and vehicle as the observer traveling at a constant speed in this scenario. Customized cars were widely utilized to reduce the shifting effects, however, the non-negligible shifting that occurred here would be common in practice as the experimental model rebuilds the real VBI situations.

Table 3. Coherence-based estimation results for diverse bridge conditions.

Case	Details	$\bar{f}_{b,1}$ (Hz)	$\hat{f}_{b,1}$ (Hz)	Frequency Shift (Hz)	$\Delta f_{b,1}$ (%)
1	Original	35.4	38.9	3.5	9.9
2	0.15L, 20kg	34.2	37.8	3.6	10.5
3	0.15L, 10kg	34.9	38.5	3.6	10.3
4	0.15L, 5kg	35.1	38.7	3.6	10.2
5	0.5L, 20kg	33.8	37.5	3.7	10.9
6	0.5L, 10kg	34.3	38.0	3.7	10.7
7	0.5L, 5kg	34.7	38.3	3.6	10.4
8	0.6L, 20kg	34.0	37.5	3.5	10.3
9	0.6L, 10kg	34.5	37.9	3.4	9.8
10	0.6L, 5kg	35.0	38.5	3.5	10

5 CONCLUSION

This paper proposes a novel strategy to identify the bridge natural frequency from a passing truck. It uses the vertical accelerations of four sensors mounted on different positions of a commercial truck only, overcoming the limitation that the vehicle-based measurement always requires tailored cars as vibration exciters to obtain bridge-relevant information. The present method can detect the bridge-related frequency from a vehicle spectrum with complicated frequency components. Experiments are performed to examine the feasibility of the present methodology, where a steel beam and a real scaled truck model in full loading condition are employed to reconstruct the actual VBI system. The following conclusions can be drawn based on the results:

(1) The present strategy can successfully identify the 1st mode frequency of the bridge by solely using vehicle vibration responses under noises from engine excitations and complicated vehicle dynamics.

(2) The bridge frequency is shown to appear as a prominent peak in the vehicle cross-spectrum with a large coherence index.

(3) The strategy performs outstandingly when using a fully loaded truck, which provides an identification success rate of 100% without requiring prior knowledge.

Nevertheless, it should be noticed that there is a non-negligible difference between the actual bridge frequency and its occurrence in the vehicle spectrum due to Doppler's effect. This is influenced by the selection of vehicles and bridges. Studies will be conducted on other types of bridges to further investigate the effectiveness of the present strategy.

6 ACKNOWLEDGMENT

This research was sponsored by the Jane and Aatos Erkko Foundation in Finland. The 1st author of this research was also financially supported by the Finnish Foundation for Technology Promotion (TES) and Chinese Scholarship Council (CSC). The last author is funded by the Academy of Finland Postdoctoral Research Project (339493). The financial support and the assistance of the laboratory staff at Aalto University are gratefully acknowledged. Any findings, opinions, conclusions, and recommendations of this paper are those of the authors and do not necessarily reflect the views of the research sponsor.

7 REFERENCES

Salawu, O.S. 1997. Detection of structural damage through changes in frequency: a review. *Engineering Structures* 22(9): 718-723.

Sohn, H., Farrar, C.R., Hemez, F.M., Shunk, D.D., Stinemates, D.W., Nadler, B.R. & Czarnecki, J.J. 2003. *A review of structural health monitoring literature: 1996–2001*. Los Alamos National Laboratory: USA.

Enckell, M., Glisic, B., Myrvoll, F. & Bergstrand, B. 2011. Evaluation of a large-scale bridge strain, temperature and crack monitoring with distributed fibre optic sensors. *Journal of Civil Structural Health Monitoring* 1(2): 37–46.

Kim, S., Pakzad, S., Culler, D., Demmel, J., Fenves, G., Glaser, S. & Turon, M. 2006. Wireless sensor networks for structural health monitoring. *Proceedings of the 4th international conference on Embedded networked sensor systems*: 427–428.

Elhattab, A., Uddin, N. & O'Brien, E. 2016. Drive-by bridge damage monitoring using bridge displacement profile difference. *J Civil Struct Health Monitor* 6(5): 839–850.

Cantero, D., McGetrick, P., Kim, C.W. & O'Brien, E. 2019. Experimental monitoring of bridge frequency evolution during the passage of vehicles with different suspension properties. *Eng Struct* 187: 209–219.

Nguyen, K.V. & Tran, H.T. 2010. Multi-cracks detection of a beam-like structure based on the on-vehicle vibration signal and wavelet analysis. *Journal of Sound and Vibration* 329(21): 4455–4465.

Miyamoto, A. & Yabe, A. 2012. Development of practical health monitoring system for short- and medium-span bridges based on vibration responses of city bus. *Journal of Civil Structural Health Monitoring* 2: 47-63.

Cerda, F., Chen, S., Bielak, J., Garrett, J., Rizzo, P. & Kovacevic, J. 2014. Indirect structural health monitoring of a simplified laboratory-scale bridge model. *Smart Structures and Systems* 13(5): 849-868.

Obrien, E.J., McGetrick, P.J. & Gonzalez, A. 2014. A drive-by inspection system via vehicle moving force identification. *Smart Struct. Syst.* 13(5): 821–848.

Obrien, E.J. & Keenahan, J. 2015. Drive-by damage detection in bridges using the apparent profile. Struct. Control. Health Monit. 22(5): 813–825.

Obrien, E.J., Fitzgerald, P.C., Malekjafarian, A. & Sevillano, E. 2017. Bridge damage detection using vehicle axle-force information. *Engineering Structures* 153: 71-80.

Nagayama, T., Reksowardojo, A.P., Su, D. & Mizutani, T. 2017. Bridge natural frequency estimation by extracting the common vibration component from the responses of two vehicles. *Engineering Structures* 150: 821-829.

Lan, Y. 2021. Improving the Drive-by bridge inspection performance by vehicle parameter optimization. *Proceedings of 8th Asia Pacific Workshop on Structural Health Monitoring (8AMWSHM)* 18: 195-202.

Lan, Y. 2021. Vertical vehicle displacement based drive-by inspection of bridge damage with parameter optimization. *Journal of Engineering Research* 9(4B): 193-210.

Hester, D. & González, A. 2017. A discussion on the merits and limitations of using drive-by monitoring to detect localised damage in a bridge. *Mechanical Systems and Signal Processing* 90: 234–253.

Wang, H., Nagayama, T. & Su, D. 2017. Vehicle Parameter Identification through Particle Filter using Bridge Responses and Estimated Profile. *Procedia Engineering* 188: 64-71.

Yang, Y., Li, Y. & Chang, K. 2014. Constructing the mode shapes of a bridge from a passing vehicle: a theoretical study. *Smart Struct Syst* 13(5): 797–819.

Malekjafarian, A., McGetrick, P. & O'Brien, E. 2015. A Review of Indirect Bridge Monitoring Using Passing Vehicles. *Shock and Vibration* 2015: 1-16.

Kim, C.W., Isemoto, R., McGetrick, P.J., Kawatani, M. & Obrien, E.J. 2014. Drive-by bridge inspection from three different approaches. *Smart Structures and Systems* 5: 775-796.

Yang, Y.B. & Yang, J.P. 2018. State-of-the-Art Review on Modal Identification and Damage Detection of Bridges by Moving Test Vehicles. *International Journal of Structural Stability and Dynamics* 18(2): 1850025.

Green, M.F. & Cebon, D. 1997. DYNAMIC INTERACTION BETWEEN HEAVY VEHICLES AND HIGHWAY BRIDGES. *Computers & Structures* 62(2): 253-264.

Liu, J., Chen, S., Bielak, J. & Garrett, J.H. 2020. Diagnosis algorithms for indirect structural health monitoring of a bridge model via dimensionality reduction. *Mechanical Systems and Signal Processing* 136: 106454.

Bendat, J.S. & Piersol, A.G. 2011. *Random data: analysis and measurement procedures*. Canada.

Zhang, Y., Miyamori, Y., Mikami, S. & Saito, T. 2019. Vibration-based structural state identification by a 1-dimensional convolutional neural network. *Computer-Aided Civil and Infrastructure Engineering* 34(9): 822-839.

Zhang, Y., Miyamori, Y., Saito, T., Mikami, S. & Oshima, T. 2019. Robustness Tests of a Vibration-based Structural State Identification Method Through a 1-D Convolutional Neural Network. *Proceedings of 9th International Conference on Structural Health Monitoring of Intelligent Infrastructure Conference (SHMII9)*. Missouri: USA.

Koski, K., Fülöp, L., Tirkkonen, T., Yabe, A. & Miyamoto, A. 2021. Heavy vehicle-based bridge health monitoring system. *Proceedings of 10th International Conference on Bridge Maintenance, Safety and Management, IABMAS 2020*. Sapporo: Japan.